Blocking glutamine transport normalizes lymphatic vessels in hypoxic environments by attenuating glycolysis

Ellie Johandes[1,2], Eva Hall[1,2], Tomas Harbut[1,2], Kaden Priebe[1,2], Margaret A. Schwarz[3,4,5], Donny Hanjaya-Putra[1,2,5,6,7]

[1] Bioengineering Graduate Program, University of Notre Dame, Notre Dame, IN 46556
[2] Aerospace and Mechanical Engineering, University of Notre Dame, Notre Dame, IN 46556
[3] Chemistry and Biochemistry, University of Notre Dame, IN 46556
[4] Cell Biology and Physiology, Indiana University School of Medicine, South Bend, IN 46556
[5] Harper Cancer Research Institute, University of Notre Dame, Notre Dame, IN 46556
[6] Chemical and Biomolecular Engineering, University of Notre Dame, Notre Dame, IN 46556
[7] Center for Stem Cell and Regenerative Medicine, University of Notre Dame, Notre Dame, IN 46556

Running Title: Glutamine is a tool to control hypoxic lymphangiogenesis

Keywords: Glycolysis, Vascular Remodeling, Lymphatic Vessels, Endothelial Cell, Hypoxia, Metabolism, Glutamine

Address correspondence to:
Donny Hanjaya-Putra
2010G McCourtney Hall East
University of Notre Dame
Notre Dame, IN 46556
Email: dputra1@nd.edu
Phone: 574-631-2291

Abstract

Dysfunctional lymphangiogenesis is a component of several diseases with hypoxic microenvironments, including secondary lymphedema and solid malignancies. These vessels are ineffective at draining interstitial fluid, resulting in complications such as increased inflammation, slowed wound healing, and, for cancer patients, increased risk of metastasis.

Current treatments to normalize vasculature have negative effects on healthy vessels and do not specifically target lymphatic endothelial cells (LECs). As hypoxia is known to change endothelial cell metabolism, exploiting LEC-specific metabolic pathways may provide a focused approach to restoring lymphatic function in patients. However, outside of glycolysis, changes to LEC metabolism in hypoxic conditions are understudied. To address this gap in knowledge, we examined the impact of glutamine availability on factors critical to lymphangiogenesis, including glycolysis, cell proliferation, and migration. We found that increasing glutamine availability results in increased lactate production as well as a hypoxia-specific increase in glycolytic genes *HK2*, *GLUT1*, and *GLUT3*. The presence of glutamine also encouraged LEC proliferation, while blocking glutamine transport reduced lactate production, *HK2* expression, and slowed collective LEC migration. In a vessel formation assay, we found that glutamine increased vessel formation in normoxic conditions, but lowered vessel connectivity in hypoxic conditions, reflecting the dysfunction seen in hypoxic diseases. However, attenuating glycolysis by blocking glutamine transport caused LECs to form longer, interconnected vascular networks. This study reveals that glutamine availability can modulate LEC glycolysis, and therefore lymphangiogenesis, in a hypoxia-dependent manner. Collectively, our study identifies glutamine availability as a potential target for lymphatic vessel normalization in chronic and hypoxic diseases.

1. Introduction

The lymphatic system is responsible for fluid balance, waste removal, and immune cell trafficking. In healthy tissues, new lymphatic vessels will sprout in response to tissue damage, driven by vascular endothelial growth factors (VEGFs), inflammation, and hypoxia (1). These vessels speed healing by draining inflammatory cytokines and resolving edema. In mice, increased lymphangiogenesis has been shown to improve cutaneous wound healing, reduce fibrosis post myocardial infarction, and protect against neurological damage from stroke (2–4). If inflammation and hypoxia persist, lymphangiogenesis can become dysfunctional. Rather than forming organized, stable vasculature, new vessels are disorganized and leaky. Impaired fluid drainage can result in edema, increased inflammation, hypoxia, fibrosis, and slowed wound healing (5). Dysfunctional lymphatics exacerbate chronic conditions such as secondary lymphedema and allergic asthma, as well as provide convenient pathways for metastasis in the solid tumor microenvironment (5–8).

Despite the importance of lymphatic vasculature, much of our current knowledge of vascular dysfunction and normalization comes from studies on blood endothelial cells (BECs) (9–11). While LECs share many similarities to BECs, including their reliance on glycolysis for energy and expression of CD31/PECAM-1, the lymphatic system's role in lymph transport gives LECs a distinct identity (12–16). Unique to LECs is their expression of prox1 and podoplanin, which are responsible for the development of lymphatic vasculature and maintenance of lymphatic identity (17–19). Their expression of LYVE-1, a hyaluronan receptor, acts as a docking site for dendritic cells and assists in the migration of macrophages (20). While both BECs and LECs can form vessels in response to vascular endothelial growth factor (VEGF)-A, VEGF-C is the main driver of lymphangiogenesis. Furthermore, compared to other endothelial cells (ECs), LECs express more genes associated with vesicular transport (21–23). In terms of behavior, LECs have different patterns of cell-cell adhesion, paracrine signaling, and methods of

contact inhibition compared to BECs (24–28). As it should not be assumed that previous techniques for vascular normalization applied to BECs will work as effectively for LECs (29), this study seeks to find new methods to curb hypoxia-driven lymphangiogenesis.

Hypoxia spurs vessel growth through the stabilization of hypoxia-inducible factors (HIFs) (30). In endothelial cells (ECs), HIFs spur vessel growth by upregulating migratory signaling pathways, increasing the production of VEGFs and their receptors (VEGFRs), and shifting cell metabolism towards increased glycolysis (31, 32). As such, VEGFR inhibitors are the main target to control vessel growth. However, anti-angiogenic treatments affect both healthy and dysfunctional vessels and risk over-pruning vasculature (11, 33). As such, researchers have turned to endothelial metabolism as a mechanism to normalize vasculature (34). Glycolysis has become a popular target due to its increase during EC migration and vessel sprouting, as well as its association with increased vascular permeability (10, 35). Previous works in BECs have demonstrated that inhibiting glycolytic enzyme PFKFB3 can inhibit vascular sprouting *in vitro* and normalize tumor vasculature for improved drug delivery in mice (36, 37). Success has also been found by co-inhibiting pyruvate dehydrogenase and glutaminase-1 (38). In LECs, reducing the translation of glycolytic enzyme hexokinase II (HK2) with miR-484 reduced pathological lymphangiogenesis in mouse corneas (39). However, given the importance of glycolysis in active and quiescent ECs, over-inhibition can result in cell death (12). Rather than targeting glycolysis directly, we instead sought to attenuate glycolysis in an LEC-targeted manner by controlling glutamine availability.

Glutamine is the most abundant amino acid in the blood. Its metabolites contribute to multiple cellular pathways in LECs and BECs, including nucleotide synthesis, lipid synthesis, glutaminolysis, and redox homeostasis (40–42). Although a direct link between glutamine availability and glycolysis has not been shown in ECs, glutamine is also highly consumed in other cell types which heavily rely on glycolysis, including lymphocytes, stem cells, and some cancers (43–48). As in glycolysis, the transcription of genes associated with glutamine metabolism are also increased in hypoxic conditions via HIF signaling, marking it as a promising target for hypoxic LECs (49, 50). Moreover, although inhibiting glutamine dehydrogenase was shown to lower both venous and lymphatic sprouting *in vitro*, it disproportionally impairs LEC migration (51)

In this study, we seek to determine whether controlling glutamine availability can influence glycolysis, and therefore lymphangiogenesis, in normoxic and hypoxic LECs. First, we clarify the relationship between glutamine availability and glycolysis by measuring glycolytic markers *HK2*, *GLUT1, GLUT3*, and lactate production over increasing concentrations of glutamine. We then repeat these experiments while pharmacologically inhibiting glutamine transport. Then, we assess glutamine metabolism as a new target for lymphatic vessel normalization by evaluating its impact on LEC proliferation, migration, and vessel formation. Our results indicate that hypoxic conditions increase the use of glutamine by LECs. The production of glucose transporters and HK2 by hypoxic LECs positively correlates with glutamine availability, as does lactate production. We also found that glutamine increases LEC proliferation and migration, while its effect on vessel formation is oxygen dependent. As such,

we find that glutamine availability can influence LEC glycolysis, making it a future target for controlling lymphangiogenesis to normalize vasculature in chronic and hypoxic diseases.

2. Materials and Methods

A full list of reagents is available in **Table S1**.

2.1 Cell Line and Culture

Human juvenile LECs derived from the dermis (PromoCell) were expanded and used between passages 5 and 8 as previously described (29, 52, 53). LECs were cultured in Endothelial Growth Medium MV2 (MV2) media with SupplementMix (PromoCell) and incubated at 37°C with 5% CO_2. Media was replaced every other day, and cells were passaged upon reaching above 80% confluency using the DetachKit (PromoCell). All cell lines were routinely tested for mycoplasma contamination and were negative throughout this study.

2.2 Cell Treatments

2.2.1 Glutamine-supplemented media

To control glutamine concentrations, L-glutamine was dissolved in low-glucose, glutamine-free DMEM with or without MV2 SupplementMix to a concentration of 20 mM. It was then hand filtered through a 0.2 µm PES membrane before being diluted to reported concentrations. Prior to glutamine treatments, LECs were glutamine-starved by incubating overnight in glutamine-free DMEM with or without MV2 SupplementMix. The media was then replaced with glutamine-supplemented DMEM for experiments.

2.2.2 Blocking glutamine transport

Glutamine transport inhibitor V-9302 was dissolved in DMSO to a concentration of 3.71 mM and then added to MV2 to a final concentration of 10 µM. Cells were treated for 48 hours before being replaced with fresh media containing V-9302 for experiments. The concentration and duration of V-9302 treatment was based on similar *in vitro* treatments in the field of cancer research (54, 55).

2.2.2 Hypoxic Culture

For hypoxic treatments, the incubator was flushed with nitrogen to achieve a final gas ratio of 94% nitrogen, 5% carbon dioxide, and 1% oxygen. Oxygen levels in media were measured with PreSens Optical Oxygen Sensor (Regensburg, Germany) to confirm that oxygen levels in the media reached < 3% O_2 (~21 mmHg pO_2) as previously described (31). Although there is no universal standard for hypoxic treatment, 3% is considered moderate hypoxia (56). Normoxic cells were cultured at ambient oxygen (approximately 19-21% O_2 or ~140 mmHg pO_2)

in a separate incubator. Unless otherwise stated, cells were incubated in normoxic or hypoxic conditions for 24 hours. See **Fig 1** for a visual representation of cell treatments.

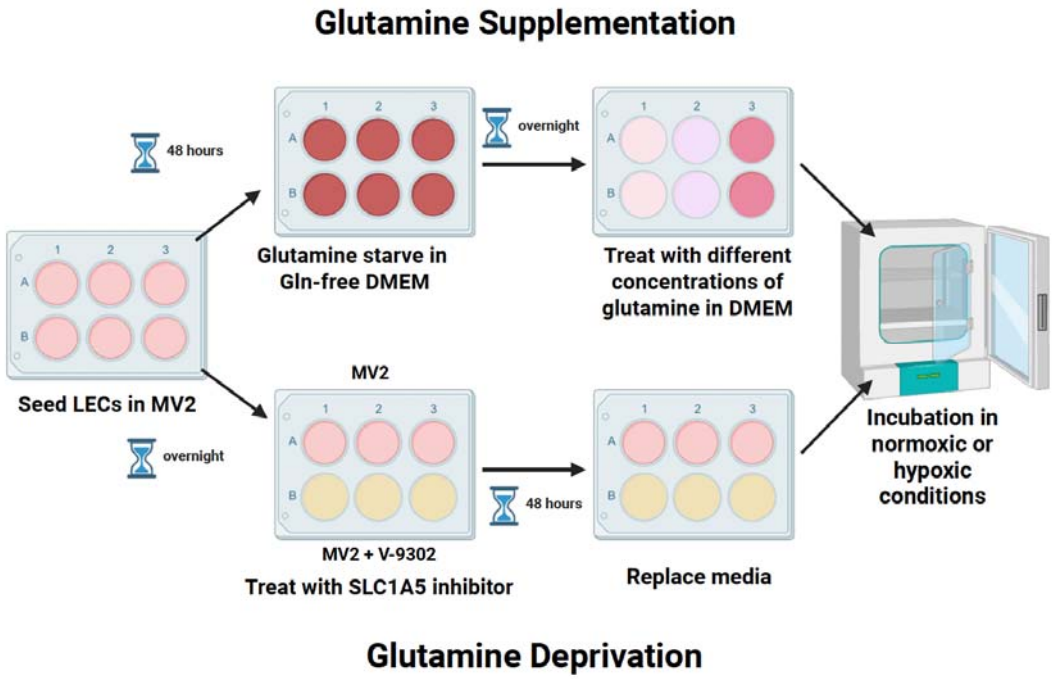

Figure 1. Illustration of Cell Treatments. Top pathway: Glutamine supplementation. Lymphatic endothelial cells (LECs) were cultured for 48 hours before being glutamine starved overnight in glutamine (Gln) free media. They were then supplemented with various concentrations of glutamine and incubated for stated times in normoxic (~21% O_2) or hypoxic (< 3% O_2) conditions. Bottom pathway: Glutamine deprivation. LECs were incubated overnight before being treated with 10 µM of V-9302, a glutamine transport inhibitor, for 48 hours. The treatment was then replaced before additional incubation in normoxic or hypoxic conditions. Image created in BioRender.

2.3 Hif1α staining and quantification

For Hif1 staining and quantification, 0.5 mL LECs in MV2 at a density of 40,000 cells/mL were seeded on top of 15mm glass coverslips in a 24 well plate and incubated for approximately 48 hours. Afterwards, the media was replaced, and the cells were cultured for an additional 24 hours in normoxic or hypoxic conditions. Prior to staining, samples were fixed in 3.7% formaldehyde for 15 minutes, permeabilized with 0.1% Triton-X for 10 minutes, and blocked in 1% Bovine Serum Albumin (BSA) in Phosphate-Buffered Saline (PBS) for 1 hour. The cells were then stained with 1:200 Mouse anti-Hif1α (Enzo Life Sciences) for 90 minutes followed by 1:500 Donkey anti-mouse 647 (Abcam) for 2 hours. Lastly, nuclei were stained with 300 nM DAPI for 3 minutes. Samples were mounted on glass slides and imaged at 10x

magnification on an Echo Revolve 2 Confocal Microscope. Quantification of nuclear Hif1α was performed in Image J2 (Version 2.14.0) using a custom program designed by our group which thresholds DAPI to create regions of interest (ROIs) for each nuclei (57). Afterwards, the fluorescent intensity of Hif1α is measured within each ROI. The individual fluorescent intensities for all nuclei were recorded across four wells for normoxic and hypoxic conditions.

2.4 Quantitative RT-PCR

For quantitative RT-PCR, 2 mL of LECs at a concentration of 40,000 cells/mL were seeded in 6-well plates and allowed to attach overnight before undergoing treatments described in **2.2.1** and **2.2.2.** The cells were lysed with Invitrogen TRIzol™ Reagent and frozen at -80□. mRNA was isolated using a RNeasy Mini Kit (Qiagen, Germantown, MD, USA). Samples were normalized to RNA concentration as measured by a Thermo Scientific NanoDrop 2000c Spectrophotometer and converted to cDNA using an Invitrogen High Capacity cDNA Reverse Transcription Kit with Rnase inhibitor. qPCR was performed using the QuantStudio 5 Real-Time PCR system. Afterwards, relative gene expression was calculated using the delta-delta Ct method, with *RPLP0* expression used as a hypoxia-stable endogenous control (58, 59). Primers for *HK2*, *GLUT1*, and *GLUT3* were sourced from Thermo Fisher Scientific TaqMan™ assays.

2.5 Lactate and glutamate production

Human LECs were seeded at a density of 10,000 cells/well in 96 well plates and allowed to attach for approximately 24 hours before being serum-starved overnight in glutamine free DMEM, MV2, or MV2 with V-9302. They were then incubated for 12 hours in normoxic or hypoxic conditions. Media was collected from each well and diluted 1:50 in PBS. Relative concentrations of glutamine and lactate in the media were then measured using Promega Lactate and Glutamate-Glo™ assays according to manufacturer instructions. Luminescence was read using a Tecan Spark plate reader, and final values were obtained after performing mean background subtraction. Wells that fell below the mean background or wells identified as outliers using Prism robust regression and outlier removal (ROUT) analysis (Q = 1%) were removed from the data set (see supporting information **Table S10.2**).

2.6 Western Blot

Human LEC samples were lysed with 1:10 RIPA buffer with 1:200 protease inhibitor. To obtain whole-cell protein, samples were centrifuged at 16,000 xg for 20 minutes, after which the supernatant was collected. Protein concentration was determined using Pierce™ Dilution-Free™ Rapid Gold BCA Protein Assay from ThermoFisher Scientific. SDS-PAGE was performed using a 12.5% acrylamide gel with 10 µg protein/lane. The protein was then transferred to a cellulose membrane. After blocking and staining, blots were imaged using an UVP ChemiDoc-It^2® Imager (Upland, CA, USA) and quantified using Image J2. Target band intensity was normalized to the intensity of RPLP0 bands. Uncropped images are available in **Fig S2**.

2.7 Proliferation assay

Human LECs were seeded at a density of 80,000 cells/mL on 12mm circular glass slides and allowed to attach for approximately 24 hours. The cells were then serum and glutamine starved in glutamine-free DMEM overnight before the media was replaced with supplemented DMEM containing 0 or 10 mM of glutamine. LECs were incubated for 24 hours in normoxic or hypoxic conditions before undergoing a proliferation assay using a Click-iT™ Plus EdU AlexaFluor™ 488 Imaging Kit (Thermo Fisher Scientific, C10637). Cell nuclei were stained with DAPI. Cells which incorporated Edu, and were therefore undergoing DNA synthesis (S-phase) at the time of fixation, displayed green fluorescence. Images were thresholded in ImageJ, and the percentage of cells in S-phase was calculated by dividing the number of nuclei displaying green fluorescence by the total number of nuclei.

2.8 Scratch assay

Ibidi 2 well cell culture inserts were placed in 24 well plates and seeded with 70µL of LECs at a density of 80,000 cells/mL in MV2 per side. An additional 0.5 mL of MV2 was added outside the insert. On day 2, the media was replaced with MV2 (control) or MV2 containing 10 µM of V-9302. On day 3, the media was replaced with serum-free MV2 (control) or serum-free MV2 + 10 µM of V-9302 and allowed to incubate overnight. On day 4, the cell culture inserts were removed, and the cells were given fresh MV2 or MV2 containing V-9302. The cells were then placed in an Agilent BioTek Lionheart Automated Microscope, where they were kept at 37□ and 5% CO_2 and imaged every 6 hours for 24 hours. The area of the wound was calculated using the manual segmentation option in the ImageJ Plugin Wound Healing Size Tool (60). The percent wound closure was then determined by dividing the area of the wound at different time points by its initial area.

2.7 Vessel formation assay

The day prior to the assay, LECs treated according to section **2.2.1** and **2.2.2** were stained with 3 µM of Invitrogen CellTracker™ Red (Thermo Fisher Scientific) for 30 minutes and then passaged. The day of, 10 µL of Matrigel was added to Ibidi 15 well µ-slides (Fitchburg, WI, USA) and cured for 2 hours at 37□. The slides were seeded with 10,000 LECs per well in 50 µL of MV2, MV2 supplemented with 5 mM glutamine, or MV2 with 10 µM of V-9302 and placed in normoxic or hypoxic incubators for 6 hours to form vessels. Images were taken at 4x magnification using an Echo Revolve 2 Confocal Microscope. Before quantification, the images were processed in Image J2 by applying the built-in Gaussian blur filter with a sigma of 5 and then manually adjusting brightness and contrast (see **Figure S5**). The processed images were then analyzed using the ImageJ Plugin Kinetic Analysis of Vasculogenesis (KAV) to quantify tube/node ratio, vessel length, and number of closed loops (61, 62).

2.8 Data availability

Data is publicly available in Figshare (see **Supporting Information)** or through author request.

3. Results

3.1. Hypoxia and glutamine availability increase glutamine utilization by LECs

Hypoxia increases glutamine uptake in skeletal stem cells, T-cells, and various cancers (49, 63, 45, 64). To observe whether this trend continues in lymphatic endothelial cells, LECs were cultured for 24 hours in a hypoxic incubator. Oxygen levels in the media were measured using a Presens optical oxygen sensor to ensure a final oxygen concentration of < 3% **(Fig 2a-b)**. Hypoxia increased Hif1α protein expression and nuclear localization **(Fig 2c-d)**. To observe the impact of hypoxia on glutamine use, serum-starved LECs were cultured in media containing different concentrations of glutamine in normoxic and hypoxic conditions. After 12 hours, media samples were collected and the relative amount of glutamate in the media were measured using a Promega Glutamate-Glo luminescence assay. As glutamine is converted to glutamate by the enzyme glutaminase (GLS), the presence of glutamate in the media indicates glutamine use by LECs. In both normoxic and hypoxic conditions, increased glutamine availability increased the amount of glutamate produced. Furthermore, hypoxia significantly increased glutamate production at all levels of glutamine supplementation **(Fig 2e)**. This indicates that both glutamine and oxygen availability influence LEC glutamine utilization.

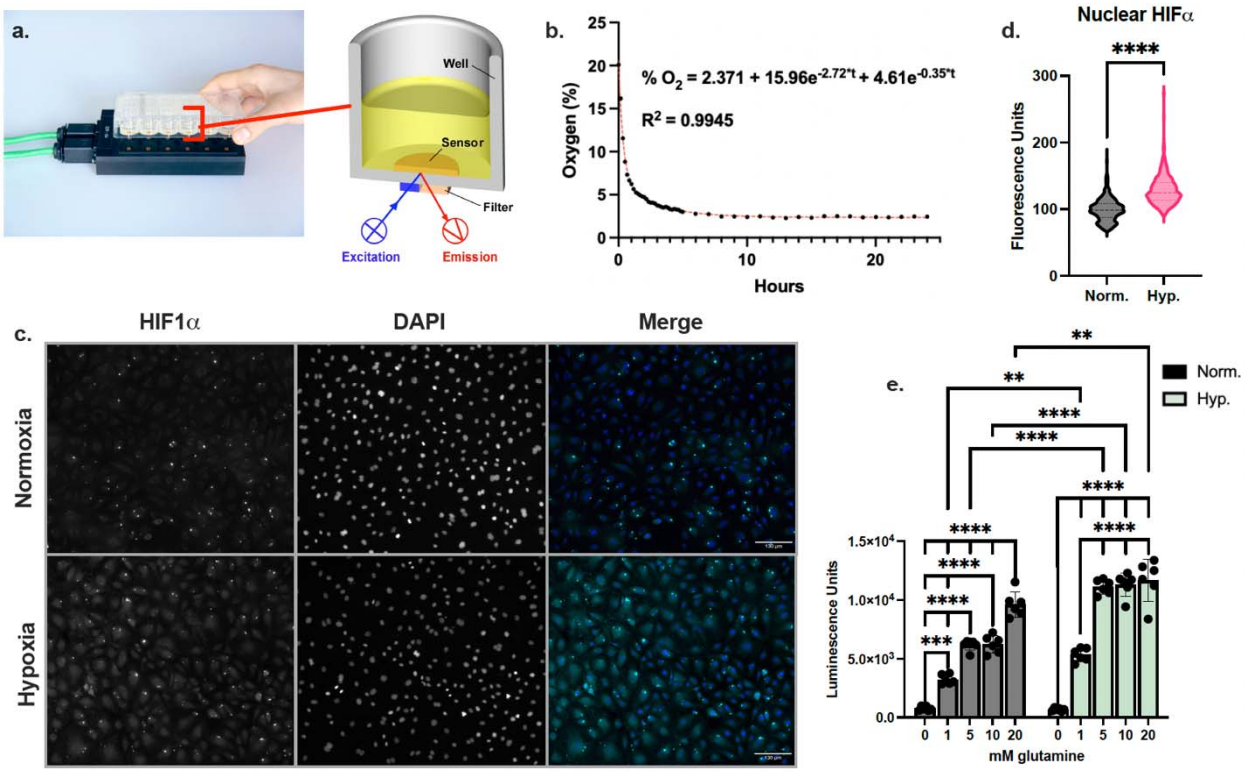

Figure 2. LEC glutamine utilization increases with both availability and hypoxia. Hypoxia was confirmed by monitoring the percent oxygen in the cell media over the incubation period as well as the increased nuclear presence of Hypoxia Inducible Factor 1α (HIF1α). **a)** PreSens SDR SensorDish™ reader and OxoHydroDish™ Plate. Images used with permission from PreSens. **b)** Percent oxygen in media over time. Oxygen diffusion from media can be modeled by a two phase decay equation (red trendline), which was calculated in Prism. **c)** LECs stained for HIF1α (cyan) after 24 hour incubation in normoxic or hypoxic conditions. Cell nuclei stained with DAPI (blue). Scale bar (white) = 130 µm. **d)** The localization of Hif1α to the nucleus was quantified by measuring the fluorescent intensity of Hif1α in regions overlapping with DAPI. n= 931 nuclei (Norm.); n = 807 nuclei (Hyp.) across 4 wells. Statistical significance determined using Student's T-test. ****P<0.0001. **e)** Glutamate in media as measured by Promega Glutamate-Glo assay after treatment with 0-20 mM of glutamine (n = 6). Glutamate is proportional to luminescence. Statistical significance determined via Two-way ANOVA with Tukey's Test. **P<0.01; ***P<0.001; ****P<0.0001.

3.2. Glutamine availability amplifies hypoxia-driven glycolysis

3.2.1 Glutamine supplementation increases glycolytic markers in hypoxic LECs

To determine the relationship between glutamine availability and glycolytic function, LECs were supplemented with glutamine before incubation in normoxic or hypoxic conditions. Glycolytic activity was assessed by the expression of Hexokinase II (HK2), Glucose Transporter

1 (GLUT1) and Glucose Transporter 3 (GLUT3) mRNA and protein, as well as the presence of lactate in the media. HK2 catalyzes the phosphorylation of glucose, which is the first and rate-limiting step in glycolysis (15, 65). GLUT1 and GLUT3 are the main glucose transporters in endothelial cells (66, 67). Furthermore, the expression of HK2, GLUT1, and GLUT3 are known to be increased by hypoxia (68–70). When assessing metabolites, lactate is the end-product of glycolysis (71, 72). Together, these markers reflect changes in glycolytic activity.

Hypoxia significantly increased the gene expression of *HK2, GLUT1,* and *GLUT3* at all concentrations of glutamine **(Fig 3a-c)**. Hypoxic LECs demonstrated consistent glutamine-dose dependent *HK2* and *GLUT1* expression, A significant increase between 1 and 20 mM of glutamine was seen for *GLUT3* expression in hypoxic LECs **(Fig 3c)**. Meanwhile, gene expression in normoxia was not significantly impacted by glutamine availability. These results suggest a positive correlation between glutamine availability and glycolytic gene expression in hypoxic conditions. Interestingly, hypoxic expression of both *GLUT1* and *GLUT3* had an initial drop in expression between 0 and 1 mM, perhaps indicating a compensatory upregulation of glucose transport when glutamine is absent, as observed in cancer cells (54).

When examining protein expression using western blot (**Fig 3d)**, cells were supplemented with 10 mM (+) or 0 mM (-) of glutamine before normoxic or hypoxic incubation. With the exception of HK2, which was significantly increased by hypoxia in the presence of

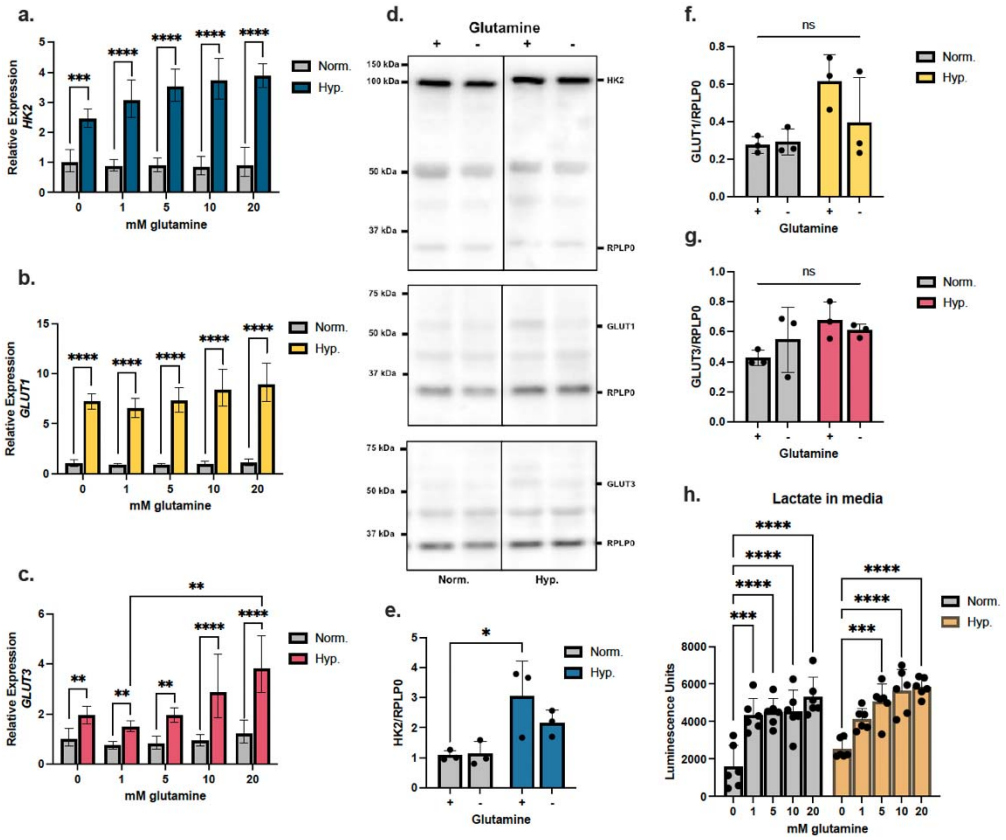

glutamine, changes in protein expression did not reach the level of statistical significance. However, hypoxic LECs supplemented with glutamine do show increased HK2, GLUT1, and GLUT3 production compared to those deprived of glutamine, reflecting changes seen at the level of gene expression **(Fig 3e-g)**. Lastly, the presence of glutamine significantly increased the presence of lactate in cell media in both normoxic and hypoxic conditions **(Fig 3h)**. Together, these results demonstrate a positive correlation between glutamine availability and glycolysis in hypoxic LECs.

Figure 3. Glutamine enhances hypoxia-induced changes to glycolytic markers. LECs were supplemented with 0-20 mM of glutamine and then incubated in normoxic (~21% O_2; Norm.) or hypoxic (< 3% O_2; Hyp.) conditions. Cells were harvested after 24 hours for gene and protein expression, while media was collected for metabolite analysis after 12 hours. Relative gene expression of **a)** *Hexokinase II (HK2)*, **b)** *Glucose Transporter 1 (GLUT1), and* **c)** *Glucose Transporter 3 (GLUT3)* was determined using the ΔΔCt method with *RPLP0* as an endogenous control. n = 3. Error bars represent upper and lower fold changes, calculated using the standard deviation of ΔCt. **d)** Western blot of HK2, GLUT1, GLUT3, and RPLP0 after treatment with 0 mM (-) or 10 mM (+) of glutamine. **e-g)** Protein expression was quantified using ImageJ and normalized to RPLP0. n = 3. **h)** Lactate in media was measured using the Promega Lactate-Glo assay, in which the amount of lactate is proportional to luminescence. n = 6. Statistical

significance for all assays was determined via Two-way ANOVA with Tukey's Test. *P<0.05; **P<0.01; ***P<0.001; ****P<0.0001.

3.2.2. Lowering glutamine uptake decreases glycolytic gene expression and lactate production.

To further define the relationship between glutamine availability and glycolysis, LECs were treated with V-9302, a competitive inhibitor of glutamine transport protein SLC1A5 (48, 73). Treatment with V-9302 significantly reduced glutamate production by hypoxic LECs, indicating a successful reduction of glutamine transport into the cell **(Fig 4a).** In hypoxic conditions, blocking glutamine transport significantly decreased lactate production **(Fig 4b)**. V-9302 treatment also resulted in non-significant reductions in hypoxic *HK2* and *GLUT1* gene

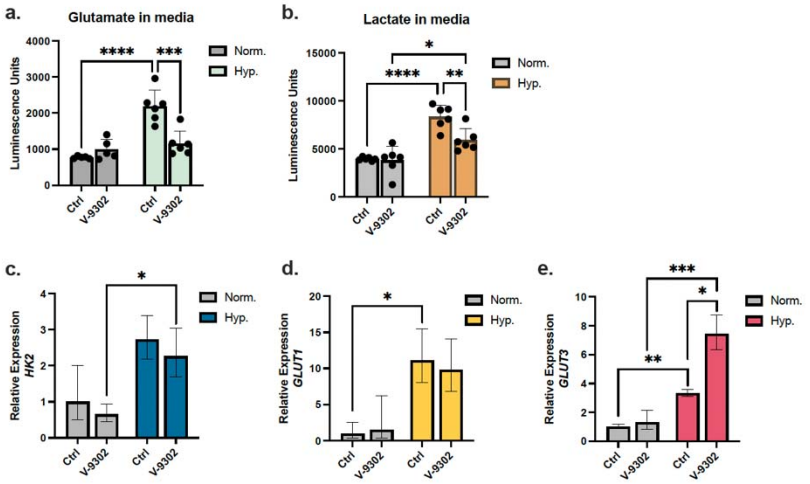

expression **(Fig 4c-d)**. Conversely, lowering glutamine transport significantly increased the hypoxic expression of *GLUT3*, supporting the idea that glucose transport is upregulated as compensation for decreased glutamine availability **(Fig 3e)**. These results suggest that glutamine supports a metabolic shift towards glycolysis in hypoxic LECs, although hypoxia remains the primary driver of this change.

Figure 4. Blocking glutamine transport lowers glycolytic indicators but increases glucose transport gene expression in hypoxic conditions. LECs were treated with 10 μM of V-9302 for 48 hours prior to treatment. Before hypoxic incubation, fresh media containing V-9302 was provided. **a)** Glutamate in media as measured by Promega Glutamate-Glo assay at 12 hours, in which luminescence is proportional to the amount of glutamate in cell media. n = 5 for normoxic conditions, n = 6 for hypoxic conditions. **b)** Lactate in media as measured by Promega Lactate-Glo assay at 12 hours. Lactate is proportional to luminescence. n = 6. **c-d)** Relative gene expression of *Hexokinase II (HK2)*, *Glucose Transporter 1 (GLUT1), and Glucose Transporter 3 (GLUT3)* was determined using the ΔΔCt method, with *RPLP0* as the endogenous control. n=3. Error bars represent upper and lower fold changes, calculated using the standard deviation of ΔCt. Statistical significance for all assays was determined via Two-way ANOVA with Tukey's Test. *P<0.05; **P<0.01; ***P<0.001; ****P<0.0001.

3.3. Glutamine causes functional changes in LECs

Having observed a positive relationship between glutamine availability and glycolysis in hypoxic LECs, we further tested how glutamine availability affects lymphatic functions known to be powered by glycolytic activity, including proliferation, migration, and vessel formation (12, 74).

3.3.1 Glutamine supports LEC proliferation and cell migration.

To investigate the effect of glutamine supplementation on LEC proliferation, we measured DNA synthesis using a ThermoFisher Click-iT™ Plus EdU AlexaFluor™ 488 Imaging Kit. Cells which incorporated EdU during DNA synthesis (S-phase) displayed green fluorescence **(Fig 5a)**. Cell proliferation was then quantified by the percentage of cells in S-phase **(Fig 5b)**. We observed that the presence of glutamine significantly increased the number of normoxic LECs in S-phase, from under 2% in glutamine-free media to 16% with glutamine. In hypoxia, the presence of glutamine increased S-phase cells from approximately 1% to 3%. Therefore, glutamine appears to offer some protection against hypoxia-induced decreases in proliferation caused by oxidative stress (75).

The impact of glutamine deprivation on collective LEC migration was observed using a wound-healing scratch assay (62). LECs (control or treated with V-9302 according to **2.2.2.**) were seeded in Ibidi two well culture inserts and allowed to grow to confluency. Upon removal of the insert, the cells were imaged every 6 hours for 24 hours using an Agilent BioTek Lionheart Automated Microscope (62). Representative images at 0, 12, and 24 hours are shown in **Fig 5c**. The area of the wound was calculated using the manual segmentation option in the ImageJ Plugin Wound Healing Size Tool (60, 62). Untreated LECs showed significantly faster wound healing than V-9302 treated cells. While untreated LECs approached full wound closure by 24 hours, LECs treated with V-9302 approached 70% wound closure **(Fig 5d)**. This result indicates that blocking glutamine transport slows collective LEC migration required for lymphatic vessel sprouting.

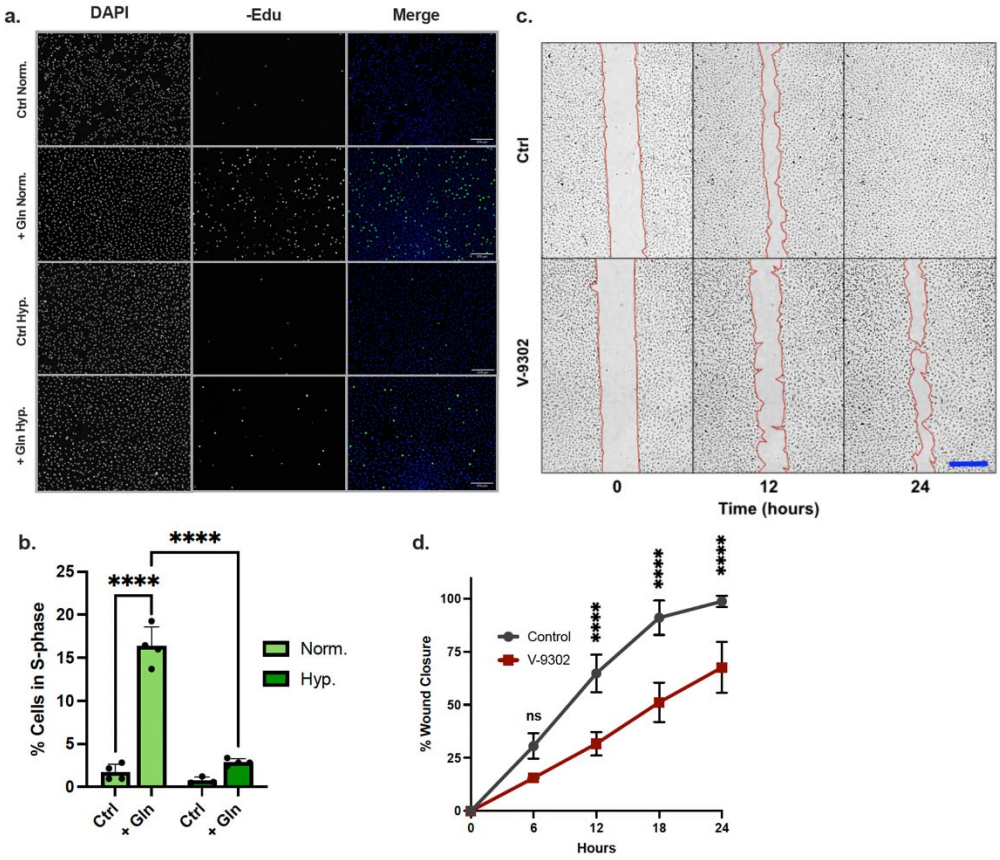

Figure 5. Glutamine increases LEC proliferation and migration. a) LEC proliferation after treatment with 0 mM (Ctrl) or 10 mM (+ Glutamine) in normoxic and hypoxic conditions. Cell nuclei were stained with DAPI (blue), while nuclei of cells in S-phase were stained green using an Invitrogen Click-It -Edu assay. Scale bar (white) = 270 µm. **b)** Cell proliferation as measured by percent cells in S-phase. n = 4. **c)** Representative images of wound healing assay in normoxic conditions at 0, 12, and 24 hours. Scale bar (blue) = 500 µm. **d)** Quantification of wound-healing assay as percent wound closure. n = 4 for control group; n = 3 for V-9302 group. Statistical significance for all quantifications determined using two-way ANOVA with Tukey's Test. *P<0.05; **P<0.01; ***P<0.001; ****P<0.0001.

3.4. Impact of glutamine on LEC tube formation oxygen-dependent

To investigate the impact of glutamine supplementation and deprivation on *in vitro* lymphatic sprouting, a 2D tube formation assay was performed (76). LECs were seeded on Matrigel in MV2 media, MV2 + 5 mM of glutamine, or MV2 + 10 µm of V-9302 and cultured for 6 hours in normoxic or hypoxic conditions. The vascular networks were then quantified with the ImageJ Plugin Kinetic Analysis of Vasculogenesis (61, 76). The average vessel length, number of closed loops, and tubes/nodes ratio were examined (52, 53, 76). Longer vessels and increased looping indicate more developed, inter-connected networks, while short vessels which form few loops indicate fragmentary vasculature (28, 53). The tubes/nodes ratio can indicate

both level of branching or fragmentation and relies on the other two metrics to provide context (62).

We found that the effect of glutamine supplementation on lymphatic tube formation was dependent on oxygen. In normoxic culture, glutamine supplementation did not change vessel length but resulted in a non-significant increase in loop formation when compared to the control. When glutamine transport was blocked using V-9302, the LECs failed to form interconnected networks (**Fig 6a)**. This resulted in shorter vessels, decrease in loop formation, and increase in tubes/node ratio **(Fig 6b-e).**

In hypoxic conditions, the opposite effect was observed. In comparison to control and V-9302 treated cells, LECs supplemented with glutamine had formed shorter vessels with fewer closed loops and higher tubes/nodes ratio (**Figure 6b-e**). LECs treated with V-9302, on the other hand, showed a morphology closer to that of the control group. This result indicates that while glutamine availability can control vascular morphology, the effect is determined by environmental conditions.

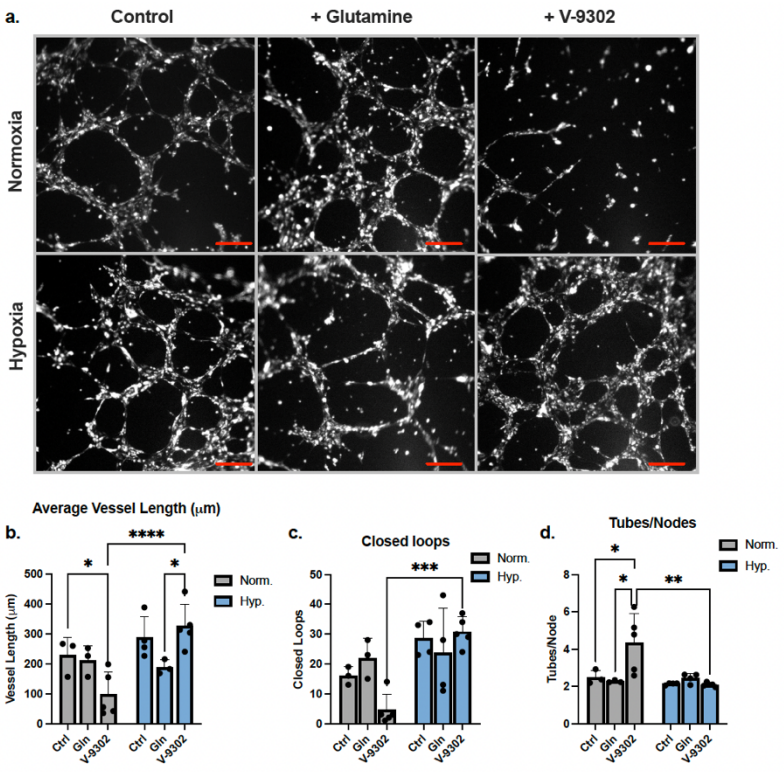

Figure 6. Impact of glutamine on LEC tube formation oxygen-dependent. Control (ctrl) or V-9302 treated LECs were stained with CellTracker Red and seeded on Matrigel in MV2, MV2 + 5 mM glutamine (Gln), or MV2 + 10 µm of V-9302. The cells were then incubated in normoxic (norm.) or hypoxic (hyp.) conditions for 6 hours. **a)** Representative images of 2D vascular networks. Scale bar (red) = 200 µm. **b-d)** Quantification of **b)** average vessel length, **c)** closed loops and **d)** tubes/nodes ratio in vascular networks using Image J Plugin Kinetic Analysis of Vasculogenesis. n = 3 norm ctrl; n = 3 norm + gln; n = 5 norm. + V-9302; n = 4 hyp. ctrl; n = 4

hyp. + gln; n = 5 hyp. + V-9302. Statistical significance determined using two-way ANOVA with Tukey's Test. *P<0.05; **P<0.01; ***P<0.001; ****P<0.0001.

4. Discussion

Glycolysis has a vast influence on lymphatic cell proliferation, migration, and lymphangiogenesis. This is especially true in hypoxic conditions, where glycolysis is further increased by a lack of oxygen for cellular respiration and the upregulation of glycolytic genes by HIF transcription factors. Therefore, small changes in glycolytic output can result in large changes to LEC behavior.

In this study, we investigated whether glutamine metabolism could influence glycolysis in hypoxic lymphatic endothelial cells. First, we showed that hypoxic conditions increase the amount of glutamate produced by LECs and therefore the amount of glutamine the cells are metabolizing. Next, we found that gene and protein expression of GLUT1, GLUT3, and HK2 increased with increasing glutamine concentrations under hypoxic conditions. LECs also produced more lactate when exposed to higher glutamine concentrations regardless of oxygen availability. The opposite effect was observed when glutamine transport was blocked using SLC1A5 inhibitor V-9302. It should be noted that lactate can also be a byproduct of glutaminolysis when glutamine is used for fatty acid synthesis, so changes in glycolysis may not be the only contributor to changes in LEC lactate production (77). Even so, the combined results indicate that glutamine availability influences glycolysis in hypoxic LECs.

Given that hypoxia is the main driver of metabolic shifts towards glycolysis, we then sought to determine if the changes to glycolysis caused by glutamine result in tangible differences in LEC behavior. For this, we examined LEC proliferation, migration, and vessel formation. We found that glutamine significantly increases LEC proliferation in normoxia and provides some protection against hypoxia-induced decreases in proliferation. This data agrees with previous studies on other endothelial cell types (78–80). We also found that blocking glutamine transport with V-9302 slows LEC migration, which coincides with Peyton et al.'s (2018) observation that glutaminase-1 stimulates the migration of endothelial cells (79). In a recent study comparing LEC and BEC metabolism, Durot et al. also found that inhibiting glutamate dehydrogenase over a 5-day period resulted in an LEC-specific decrease in cell migration, which was then rescued with dimethyl-α-ketoglutarate supplementation (81). It should be noted that Kim et al. (2017) did not report a link between glutamine and endothelial cell migration (78). This alternative finding could be attributed to differences in cell culture and treatments, and it points to the need to confirm these results *in vivo*.

Lastly, we examined the impact of glutamine supplementation and deprivation on lymphatic tube formation. While glutamine increased network formation in normoxic conditions, increasing glutamine availability in hypoxic conditions led to the generation of thinner tubes with less connectivity. This result was reversed with V-9302 treatment. We hypothesize that these changes in morphology are due to glutamine's influence on the glycolytic activity of the cells. Hypoxia increases endothelial cell glycolysis through the HIF1α pathway, leading to the

increased network formation seen in the control group. When glycolysis is further increased with glutamine supplementation, the rate of LEC migration increases as seen in **Fig 5c-d**, leading to thinner vessels. V-9302 attenuates any glutamine-induced increases to glycolysis, causing the vessel morphology of hypoxic LECs treated with V-9302 to reflect the control hypoxia group. This could also explain why glutamine supplementation increases vessel formation in normoxia, although any changes in glycolysis caused by glutamine in normoxic conditions were not observed at the level of gene or protein expression **(Fig 3**).

While this study did not explore the mechanism by which glutamine availability influences LEC glycolysis, recent work by Han et al. (2025) has uncovered that glycolysis and glutamine metabolism are both controlled by mTORC1 through Myc-HK2/GLS signaling during lymphatic development (82). Other metabolic studies have shown that glutamine and glutaminolysis activates mTORC1 (83–85). Another potential mechanism involves glutamine's role in redox homeostasis. While excessive reactive oxygen species (ROS) can inhibit glycolysis, glutathione, a metabolite of glutamine, can scavenge ROS. Therefore, increased glutamine flux in hypoxic conditions may relieve ROS inhibition of glycolysis (86). Future studies *in vivo* will be needed to confirm these relationships, as well as the ability of glutamine to influence glycolysis at concentrations that reflect those found in human plasma, approximately 0.4 - 0.9 mM (87–89).

This study identifies glutamine as a supporter of lymphatic endothelial cell glycolysis under hypoxic conditions **(Fig 7)**. It is a viable tool to modulate lymphatic endothelial cell proliferation, migration, and vessel formation in normoxic and hypoxic conditions. Collectively, this work provides evidence that indirect targeting of lymphatic endothelial cell glycolysis though alternate metabolic pathways is a viable method to control lymphangiogenesis. Potential applications include using glutamine to improve lymphatic vascularization in tissue models or spur wound healing in otherwise healthy tissues. Reducing glutamine uptake, on the other hand, could be used to normalize lymphatic vasculature in diseases with chronic hypoxia, such as solid malignancies or secondary lymphedema, without having the side effects associated with anti-VEGF therapies.

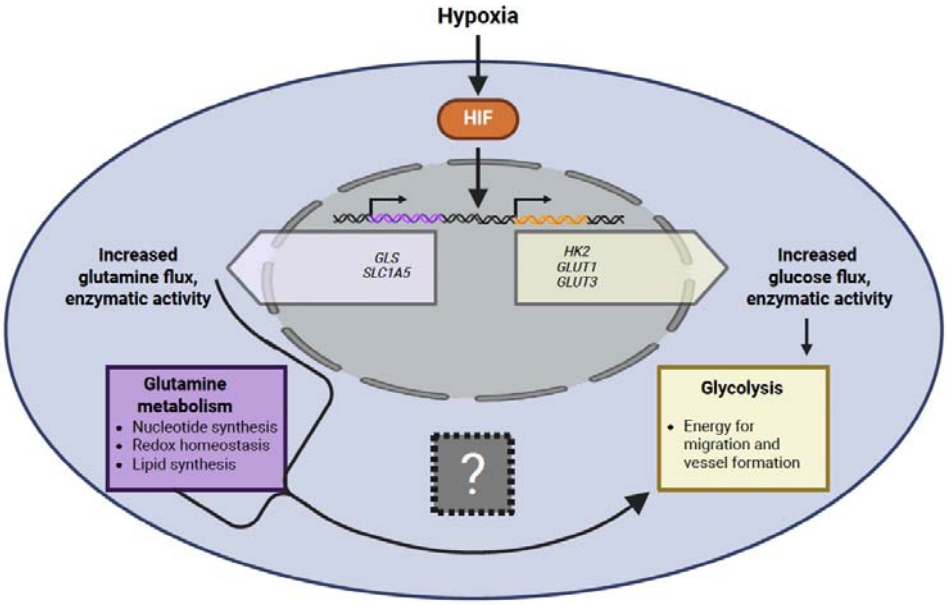

Figure 7. Summary of relationship between glutamine and glycolysis in hypoxic LECs. Hypoxia stabilizes HIF transcription factors, which increase the transcription of genes related to glutamine metabolism as well as glycolysis. Increased glutamine flux into LECs provides increased nucleotide synthesis, lipid synthesis, and scavenging of reactive oxygen species through glutamine's metabolites. This process supports glycolysis through a currently undetermined mechanism. Image made in BioRender.

Supporting Information

Supporting information is available at: Johandes, Ellie (2025). Supporting Information Glutamine Availability Impacts Lymphatic Endothelial Cell Glycolysis and Lymphangiogenesis in Hypoxic Environments. figshare. Preprint. https://doi.org/10.6084/m9.figshare.30913952.v2

Acknowledgments

We acknowledge support from the University of Notre Dame through "Advancing Our Vision" Initiative in Stem Cell Research, Harper Cancer Research Institute – American Cancer Society Institutional Research Grant (IRG-17-182-04), American Heart Association through Career Development Award (19-CDA-34630012 to D.H.-P.), National Science Foundation (2047903 and 2225601 to D.H-P.), and the National Institutes of Health (1R35-GM-143055 to D.H.-P.).

Conflicts of interest

The authors declare no conflicts of interest

Author Contributions

E.J., D.H.P., E.H. and M.S. conceived and planned the experiments. E.J. carried out experiments, conducted data analysis, and wrote the manuscript. E.H. designed the ImageJ code to quantify fluorescence in the nucleus of individual cells. T.H. and K.P. assisted in conducting experiments. All authors contributed to data interpretation and editing the manuscript.

References

1. Zampell, J. C., Yan, A., Avraham, T., Daluvoy, S., Weitman, E. S., and Mehrara, B. J. (2012) HIF-1α coordinates lymphangiogenesis during wound healing and in response to inflammation. *FASEB J.* **26**, 1027–1039
2. Pollack, B. L., Torrisi, J. S., Hespe, G. E., Ashokan, G., Shin, J., Mehrara, B. J., and Kataru, R. P. (2025) Inhibition of Th2 Differentiation Accelerates Chronic Wound Healing by Facilitating Lymphangiogenesis. *Biomedicines*. **13**, 1026
3. Vieira, J. M., Norman, S., Villa del Campo, C., Cahill, T. J., Barnette, D. N., Gunadasa-Rohling, M., Johnson, L. A., Greaves, D. R., Carr, C. A., Jackson, D. G., and Riley, P. R. The cardiac lymphatic system stimulates resolution of inflammation following myocardial infarction. *J. Clin. Invest.* **128**, 3402–3412
4. Boisserand, L. S. B., Geraldo, L. H., Bouchart, J., El Kamouh, M.-R., Lee, S., Sanganahalli, B. G., Spajer, M., Zhang, S., Lee, S., Parent, M., Xue, Y., Skarica, M., Yin, X., Guegan, J., Boyé, K., Saceanu Leser, F., Jacob, L., Poulet, M., Li, M., Liu, X., Velazquez, S. E., Singhabahu, R., Robinson, M. E., Askenase, M. H., Osherov, A., Sestan, N., Zhou, J., Alitalo, K., Song, E., Eichmann, A., Sansing, L. H., Benveniste, H., Hyder, F., and Thomas, J.-L. (2024) VEGF-C prophylaxis favors lymphatic drainage and modulates neuroinflammation in a stroke model. *J. Exp. Med.* **221**, e20221983
5. Jiang, X., Tian, W., Kim, D., McQuiston, A. S., Vinh, R., Rockson, S. G., Semenza, G. L., and Nicolls, M. R. (2022) Hypoxia and Hypoxia-Inducible Factors in Lymphedema. *Front. Pharmacol.* [online] https://www.frontiersin.org/articles/10.3389/fphar.2022.851057 (Accessed December 26, 2023)
6. Ji, H., Hu, C., Yang, X., Liu, Y., Ji, G., Ge, S., Wang, X., and Wang, M. (2023) Lymph node metastasis in cancer progression: molecular mechanisms, clinical significance and therapeutic interventions. *Signal Transduct. Target. Ther.* **8**, 1–33
7. Gomez Medellin, J., Ung, T., Hollinger, M., Kurtanich, T., Blaine, K., Rosenberg, J., Wang, T., Magold, A., Ankenbruck, N., and Quandt, J. (2024) Pulmonary lymphatic endothelial cells mediate induction of bronchus associated lymphoid tissue in chronic allergic asthma. *J. Immunol.* **212**, 1054_4147-1054_4147
8. Qiu, C., Tang, C., Tang, Y., Su, K., Chai, X., Zhan, Z., Niu, X., and Li, J. (2024) RGS5+ lymphatic endothelial cells facilitate metastasis and acquired drug resistance of breast cancer through oxidative stress-sensing mechanism. *Drug Resist. Updat.* 10.1016/j.drup.2024.101149
9. Cao, H., Yu, D., Yan, X., Wang, B., Yu, Z., Song, Y., and Sheng, L. (2019) Hypoxia destroys the microstructure of microtubules and causes dysfunction of endothelial cells via the PI3K/Stathmin1 pathway. *Cell Biosci.* **9**, 20

10. Yang, K., Fan, M., Wang, X., Xu, J., Wang, Y., Gill, P. S., Ha, T., Liu, L., Hall, J. V., Williams, D. L., and Li, C. (2022) Lactate induces vascular permeability via disruption of VE-cadherin in endothelial cells during sepsis. *Sci. Adv.* **8**, eabm8965
11. Choi, Y., and Jung, K. (2023) Normalization of the tumor microenvironment by harnessing vascular and immune modulation to achieve enhanced cancer therapy. *Exp. Mol. Med.* **55**, 2308–2319
12. De Bock, K., Georgiadou, M., Schoors, S., Kuchnio, A., Wong, B. W., Cantelmo, A. R., Quaegebeur, A., Ghesquière, B., Cauwenberghs, S., Eelen, G., Phng, L.-K., Betz, I., Tembuyser, B., Brepoels, K., Welti, J., Geudens, I., Segura, I., Cruys, B., Bifari, F., Decimo, I., Blanco, R., Wyns, S., Vangindertael, J., Rocha, S., Collins, R. T., Munck, S., Daelemans, D., Imamura, H., Devlieger, R., Rider, M., Van Veldhoven, P. P., Schuit, F., Bartrons, R., Hofkens, J., Fraisl, P., Telang, S., Deberardinis, R. J., Schoonjans, L., Vinckier, S., Chesney, J., Gerhardt, H., Dewerchin, M., and Carmeliet, P. (2013) Role of PFKFB3-driven glycolysis in vessel sprouting. *Cell*. **154**, 651–663
13. De Bock, K., Georgiadou, M., and Carmeliet, P. (2013) Role of Endothelial Cell Metabolism in Vessel Sprouting. *Cell Metab.* **18**, 634–647
14. Culic, O., Gruwel, M. L., and Schrader, J. (1997) Energy turnover of vascular endothelial cells. *Am. J. Physiol.-Cell Physiol.* **273**, C205–C213
15. Yu, P., Wilhelm, K., Dubrac, A., Tung, J. K., Alves, T. C., Fang, J. S., Xie, Y., Zhu, J., Chen, Z., De Smet, F., Zhang, J., Jin, S.-W., Sun, L., Sun, H., Kibbey, R. G., Hirschi, K. K., Hay, N., Carmeliet, P., Chittenden, T. W., Eichmann, A., Potente, M., and Simons, M. (2017) FGF-dependent metabolic control of vascular development. *Nature*. **545**, 224–228
16. Muller, W. A., Ratti, C. M., McDonnell, S. L., and Cohn, Z. A. (1989) A human endothelial cell-restricted, externally disposed plasmalemmal protein enriched in intercellular junctions. *J. Exp. Med.* **170**, 399–414
17. Cha, B., Geng, X., Mahamud, Md. R., Jenny Y. Zhang, Chen, L., Kim, W., Jho, E., Kim, Y., Choi, D., Dixon, J. B., Chen, H., Hong, Y.-K., Olson, L., Kim, T. H., Merrill, B. J., Davis, M. J., and Srinivasan, R. S. (2018) Complementary Wnt Sources Regulate Lymphatic Vascular Development via PROX1-Dependent Wnt/β-Catenin Signaling. *Cell Rep.* **25**, 571-584.e5
18. Wang, Y., Keshavarz, M., Barhouse, P., and Smith, Q. (2023) Strategies for Regenerative Vascular Tissue Engineering. *Adv. Biol.* **7**, 2200050
19. Hong, Y.-K., Harvey, N., Noh, Y.-H., Schacht, V., Hirakawa, S., Detmar, M., and Oliver, G. (2002) Prox1 is a master control gene in the program specifying lymphatic endothelial cell fate. *Dev. Dyn.* **225**, 351–357
20. Jackson, D. G. (2019) Hyaluronan in the lymphatics: The key role of the hyaluronan receptor LYVE-1 in leucocyte trafficking. *Matrix Biol.* **78–79**, 219–235
21. Podgrabinska, S., Braun, P., Velasco, P., Kloos, B., Pepper, M. S., Jackson, D. G., and Skobe, M. (2002) Molecular characterization of lymphatic endothelial cells. *Proc. Natl. Acad. Sci.* **99**, 16069–16074
22. Nelson, G. M., Padera, T. P., Garkavtsev, I., Shioda, T., and Jain, R. K. (2007) Differential Gene Expression of Primary Cultured Lymphatic and Blood Vascular Endothelial Cells. *Neoplasia N. Y. N.* **9**, 1038–1045

23. Lee, C., Kim, M.-J., Kumar, A., Lee, H.-W., Yang, Y., and Kim, Y. (2025) Vascular endothelial growth factor signaling in health and disease: from molecular mechanisms to therapeutic perspectives. *Signal Transduct. Target. Ther.* **10**, 170
24. Kriehuber, E., Breiteneder-Geleff, S., Groeger, M., Soleiman, A., Schoppmann, S. F., Stingl, G., Kerjaschki, D., and Maurer, D. (2001) Isolation and Characterization of Dermal Lymphatic and Blood Endothelial Cells Reveal Stable and Functionally Specialized Cell Lineages. *J. Exp. Med.* **194**, 797–808
25. Jeong, D., Hall, E., Neu, E., and Putra, D. (2022) Podoplanin is Responsible for the Distinct Blood and Lymphatic Capillaries. *Cell. Mol. Bioeng.* 10.1007/s12195-022-00730-2
26. Carlantoni, C., Liekfeld, L. M. H., Beerens, M., and Frye, M. (2025) Same same but different? How blood and lymphatic vessels induce cell contact inhibition. *Biochem. Soc. Trans.* **53**, BST20240573
27. Lee, E., Chan, S.-L., Lee, Y., Polacheck, W. J., Kwak, S., Wen, A., Nguyen, D.-H. T., Kutys, M. L., Alimperti, S., Kolarzyk, A. M., Kwak, T. J., Eyckmans, J., Bielenberg, D. R., Chen, H., and Chen, C. S. (2023) A 3D biomimetic model of lymphatics reveals cell–cell junction tightening and lymphedema via a cytokine-induced ROCK2/JAM-A complex. *Proc. Natl. Acad. Sci.* **120**, e2308941120
28. Jeong, D. P. and P., Daniel Montes and Chang, Hsueh-Chia and Hanjaya-Putra, Donny (2023) Fractal dimension to characterize interactions between blood and lymphatic endothelial cells. *Phys. Biol.*
29. Saha, S., Fan, F., Alderfer, L., Graham, F., Hall, E., and Hanjaya-Putra, D. (2023) Synthetic hyaluronic acid coating preserves the phenotypes of lymphatic endothelial cells. *Biomater. Sci.* **11**, 7346–7357
30. Wang, G. L., Jiang, B. H., Rue, E. A., and Semenza, G. L. (1995) Hypoxia-inducible factor 1 is a basic-helix-loop-helix-PAS heterodimer regulated by cellular O2 tension. *Proc. Natl. Acad. Sci.* **92**, 5510–5514
31. Abaci, H. E., Truitt, R., Luong, E., Drazer, G., and Gerecht, S. (2010) Adaptation to oxygen deprivation in cultures of human pluripotent stem cells, endothelial progenitor cells, and umbilical vein endothelial cells. *Am. J. Physiol.-Cell Physiol.* **298**, C1527–C1537
32. Liu, L., Yu, J., Liu, Y., Xie, L., Hu, F., and Liu, H. (2025) Hypoxia-driven angiogenesis and metabolic reprogramming in vascular tumors. *Front. Cell Dev. Biol.* **13**, 1572909
33. Goel, S., Duda, D. G., Xu, L., Munn, L. L., Boucher, Y., Fukumura, D., and Jain, R. K. (2011) Normalization of the Vasculature for Treatment of Cancer and Other Diseases. *Physiol. Rev.* **91**, 1071–1121
34. Li, X., Sun, X., and Carmeliet, P. (2019) Hallmarks of Endothelial Cell Metabolism in Health and Disease. *Cell Metab.* **30**, 414–433
35. Gallemit, P. E. M., Yoodee, S., Malaitad, T., and Thongboonkerd, V. (2021) Epigallocatechin-3-gallate plays more predominant roles than caffeine for inducing actin-crosslinking, ubiquitin/proteasome activity and glycolysis, and suppressing angiogenesis features of human endothelial cells. *Biomed. Pharmacother.* **141**, 111837
36. Abdali, A., Baci, D., Damiani, I., Belloni, F., De Dominicis, C., Gelmi, M. L., Corsini, A., and Bellosta, S. (2021) In vitro angiogenesis inhibition with selective compounds targeting the key glycolytic enzyme PFKFB3. *Pharmacol. Res.* **168**, 105592

37. Cantelmo, A. R., Conradi, L.-C., Brajic, A., Goveia, J., Kalucka, J., Pircher, A., Chaturvedi, P., Hol, J., Thienpont, B., Teuwen, L.-A., Schoors, S., Boeckx, B., Vriens, J., Kuchnio, A., Veys, K., Cruys, B., Finotto, L., Treps, L., Stav-Noraas, T. E., Bifari, F., Stapor, P., Decimo, I., Kampen, K., De Bock, K., Haraldsen, G., Schoonjans, L., Rabelink, T., Eelen, G., Ghesquière, B., Rehman, J., Lambrechts, D., Malik, A. B., Dewerchin, M., and Carmeliet, P. (2016) INHIBITION OF THE GLYCOLYTIC ACTIVATOR PFKFB3 IN ENDOTHELIAL CELLS INDUCES TUMOR VESSEL NORMALIZATION, IMPAIRS METASTASIS AND IMPROVES CHEMOTHERAPY. *Cancer Cell*. **30**, 968–985
38. Schoonjans, C. A., Mathieu, B., Joudiou, N., Zampieri, L. X., Brusa, D., Sonveaux, P., Feron, O., and Gallez, B. (2020) Targeting Endothelial Cell Metabolism by Inhibition of Pyruvate Dehydrogenase Kinase and Glutaminase-1. *J. Clin. Med.* **9**, 3308
39. Zhang, Z., Ye, F., Zhang, H., Li, X., Mu, W., Li, K., and Yan, B. (2025) Reprogramming lymphatic endothelial glucose metabolism for the treatment of lymphangiogenesis-related disease. *Pharmacol. Res.* **218**, 107827
40. Teuwen, L.-A., Geldhof, V., and Carmeliet, P. (2019) How glucose, glutamine and fatty acid metabolism shape blood and lymph vessel development. *Dev. Biol.* **447**, 90–102
41. Mirveis, Z., Howe, O., Cahill, P., Patil, N., and Byrne, H. J. (2023) Monitoring and modelling the glutamine metabolic pathway: a review and future perspectives. *Metabolomics*. **19**, 67
42. Yoo, H. C., Yu, Y. C., Sung, Y., and Han, J. M. (2020) Glutamine reliance in cell metabolism. *Exp. Mol. Med.* **52**, 1496–1516
43. Carr, E. L., Kelman, A., Wu, G. S., Gopaul, R., Senkevitch, E., Aghvanyan, A., Turay, A. M., and Frauwirth, K. A. (2010) Glutamine Uptake and Metabolism Are Coordinately Regulated by ERK/MAPK during T Lymphocyte Activation. *J. Immunol.* **185**, 1037–1044
44. Tohyama, S., Fujita, J., Hishiki, T., Matsuura, T., Hattori, F., Ohno, R., Kanazawa, H., Seki, T., Nakajima, K., Kishino, Y., Okada, M., Hirano, A., Kuroda, T., Yasuda, S., Sato, Y., Yuasa, S., Sano, M., Suematsu, M., and Fukuda, K. (2016) Glutamine Oxidation Is Indispensable for Survival of Human Pluripotent Stem Cells. *Cell Metab.* **23**, 663–674
45. Loopmans, S., Tournaire, G., Stockmans, I., Stegen, S., and Carmeliet, G. (2024) Hypoxia rewires glucose and glutamine metabolism in different sources of skeletal stem and progenitor cells similarly, except for pyruvate. *J. Bone Miner. Res. Off. J. Am. Soc. Bone Miner. Res.* **39**, 150–160
46. Pérez-Escuredo, J., Dadhich, R. K., Dhup, S., Cacace, A., Van Hée, V. F., De Saedeleer, C. J., Sboarina, M., Rodriguez, F., Fontenille, M.-J., Brisson, L., Porporato, P. E., and Sonveaux, P. (2016) Lactate promotes glutamine uptake and metabolism in oxidative cancer cells. *Cell Cycle*. **15**, 72–83
47. Zhang, Z., Liu, R., Shuai, Y., Huang, Y., Jin, R., Wang, X., and Luo, J. (2020) ASCT2 (SLC1A5)-dependent glutamine uptake is involved in the progression of head and neck squamous cell carcinoma. *Br. J. Cancer*. **122**, 82–93
48. van Geldermalsen, M., Wang, Q., Nagarajah, R., Marshall, A. D., Thoeng, A., Gao, D., Ritchie, W., Feng, Y., Bailey, C. G., Deng, N., Harvey, K., Beith, J. M., Selinger, C. I., O'Toole, S. A., Rasko, J. E. J., and Holst, J. (2016) ASCT2/SLC1A5 controls glutamine uptake and tumour growth in triple-negative basal-like breast cancer. *Oncogene*. **35**, 3201–3208

49. Sun, R. C., and Denko, N. C. (2014) Hypoxic regulation of glutamine metabolism through HIF1 and SIAH2 supports lipid synthesis that is necessary for tumor growth. *Cell Metab.* **19**, 285–292
50. Xiang, L., Mou, J., Shao, B., Wei, Y., Liang, H., Takano, N., Semenza, G. L., and Xie, G. (2019) Glutaminase 1 expression in colorectal cancer cells is induced by hypoxia and required for tumor growth, invasion, and metastatic colonization. *Cell Death Dis.* **10**, 40
51. Durot, S., Doubleday, P. F., Schulla, L., Sabine, A., Petrova, T. V., and Zamboni, N. (2026) Multi-omics analysis reveals metabolic diversity underlying endothelial cell functions. *Life Sci. Alliance*. 10.26508/lsa.202503526
52. Alderfer, L., Saha, S., Fan, F., Wu, J., Littlepage, L. E., and Hanjaya-Putra, D. (2024) Multi-parameter tunable synthetic matrix for engineering lymphatic vessels. *Commun. Biol.* **7**, 1262
53. Montes, D., Saha, S., Taglione, A., Jeong, D. P., Chen, L., Fan, F., Chang, H.-C., and Hanjaya-Putra, D. (2025) Tuning the Morphological Properties of Granular Hydrogels to Control Lymphatic Capillary Formation. *Adv. Mater. Interfaces*. **12**, 2401037
54. Schulte, M. L., Fu, A., Zhao, P., Li, J., Geng, L., Smith, S. T., Kondo, J., Coffey, R. J., Johnson, M. O., Rathmell, J. C., Sharick, J. T., Skala, M. C., Smith, J. A., Berlin, J., Washington, M. K., Nickels, M. L., and Manning, H. C. (2018) Pharmacological Blockade of ASCT2-dependent Glutamine Transport Leads To Anti-tumor Efficacy in Preclinical Models. *Nat. Med.* **24**, 194–202
55. Edwards, D. N., Ngwa, V. M., Raybuck, A. L., Wang, S., Hwang, Y., Kim, L. C., Cho, S. H., Paik, Y., Wang, Q., Zhang, S., Manning, H. C., Rathmell, J. C., Cook, R. S., Boothby, M. R., and Chen, J. (2021) Selective glutamine metabolism inhibition in tumor cells improves antitumor T lymphocyte activity in triple-negative breast cancer. *J. Clin. Invest.* 10.1172/JCI140100
56. Vásquez Vélez, I. C., Charris Domínguez, C. M., Fernández Sánchez, M. J., and Garavito-Aguilar, Z. V. (2025) Hypoxia and Tissue Regeneration: Adaptive Mechanisms and Therapeutic Opportunities. *Int. J. Mol. Sci.* **26**, 9272
57. Hall, E. (2025) ROSAnalysis. [online] https://github.com/ehall8-bioe/ROSAnalysis (Accessed November 28, 2025)
58. Lafont, J. E., Talma, S., Hopfgarten, C., and Murphy, C. L. (2008) Hypoxia Promotes the Differentiated Human Articular Chondrocyte Phenotype through SOX9-dependent and -independent Pathways*. *J. Biol. Chem.* **283**, 4778–4786
59. Bence, M., Kereszturi, E., Mozes, V., Sasvari-Szekely, M., and Keszler, G. (2009) Hypoxia-induced transcription of dopamine D3 and D4 receptors in human neuroblastoma and astrocytoma cells. *BMC Neurosci.* **10**, 92
60. Suarez-Arnedo, A., Torres Figueroa, F., Clavijo, C., Arbeláez, P., Cruz, J. C., and Muñoz-Camargo, C. (2020) An image J plugin for the high throughput image analysis of in vitro scratch wound healing assays. *PLoS ONE*. **15**, e0232565
61. Varberg, K., Winfree, S., Dunn, K., and Haneline, L. (2018) Kinetic Analysis of Vasculogenesis Quantifies Dynamics of Vasculogenesis and Angiogenesis In Vitro. *J. Vis. Exp.* 10.3791/57044

62. Bui, L., Edwards, S., Hall, E., Alderfer, L., Round, K., Owen, M., Sainaghi, P., Zhang, S., Nallathamby, P. D., Haneline, L. S., and Hanjaya-Putra, D. (2022) Engineering bioactive nanoparticles to rejuvenate vascular progenitor cells. *Commun. Biol.* **5**, 635
63. Yoo, H. C., Park, S. J., Nam, M., Kang, J., Kim, K., Yeo, J. H., Kim, J.-K., Heo, Y., Lee, H. S., Lee, M. Y., Lee, C. W., Kang, J. S., Kim, Y.-H., Lee, J., Choi, J., Hwang, G.-S., Bang, S., and Han, J. M. (2020) A Variant of SLC1A5 Is a Mitochondrial Glutamine Transporter for Metabolic Reprogramming in Cancer Cells. *Cell Metab.* **31**, 267-283.e12
64. Wik, J. A., Chowdhury, A., Kolan, S., Bastani, N. E., Li, G., Alam, K., Grimolizzi, F., and Skålhegg, B. S. (2022) Endogenous glutamine is rate-limiting for anti-CD3 and anti-CD28 induced CD4+ T-cell proliferation and glycolytic activity under hypoxia and normoxia. *Biochem. J.* **479**, 1221–1235
65. Roberts, D. J., and Miyamoto, S. (2015) Hexokinase II integrates energy metabolism and cellular protection: Akting on mitochondria and TORCing to autophagy. *Cell Death Differ.* **22**, 248–257
66. Holman, G. D. (2020) Structure, function and regulation of mammalian glucose transporters of the SLC2 family. *Pflüg. Arch. - Eur. J. Physiol.* **472**, 1155–1175
67. Wu, W.-Z., and Bai, Y.-P. (2023) Endothelial GLUTs and vascular biology. *Biomed. Pharmacother.* **158**, 114151
68. Riddle, S. R., Ahmad, A., Ahmad, S., Deeb, S. S., Malkki, M., Schneider, B. K., Allen, C. B., and White, C. W. (2000) Hypoxia induces hexokinase II gene expression in human lung cell line A549. *Am. J. Physiol.-Lung Cell. Mol. Physiol.* **278**, L407–L416
69. Chen, C., Pore, N., Behrooz, A., Ismail-Beigi, F., and Maity, A. (2001) Regulation of glut1 mRNA by hypoxia-inducible factor-1. Interaction between H-ras and hypoxia. *J. Biol. Chem.* **276**, 9519–9525
70. Ryniawec, J. M., Coope, M. R., Loertscher, E., Bageerathan, V., de Oliveira Pessoa, D., Warfel, N. A., Cress, A. E., Padi, M., and Rogers, G. C. (2022) GLUT3/SLC2A3 Is an Endogenous Marker of Hypoxia in Prostate Cancer Cell Lines and Patient-Derived Xenograft Tumors. *Diagnostics*. **12**, 676
71. Rogatzki, M. J., Ferguson, B. S., Goodwin, M. L., and Gladden, L. B. (2015) Lactate is always the end product of glycolysis. *Front. Neurosci.* **9**, 22
72. Li, X., Yang, Y., Zhang, B., Lin, X., Fu, X., An, Y., Zou, Y., Wang, J.-X., Wang, Z., and Yu, T. (2022) Lactate metabolism in human health and disease. *Signal Transduct. Target. Ther.* **7**, 305
73. Schulte, M. L., Khodadadi, A. B., Cuthbertson, M. L., Smith, J. A., and Manning, H. C. (2016) 2-amino-4-bis(aryloxybenzyl)aminobutanoic acids: a novel Scaffold for inhibition of ASCT2-mediated glutamine transport. *Bioorg. Med. Chem. Lett.* **26**, 1044–1047
74. Wu, D., Harrison, D. L., Szasz, T., Yeh, C.-F., Shentu, T.-P., Meliton, A., Huang, R.-T., Zhou, Z., Mutlu, G. M., Huang, J., and Fang, Y. (2021) Single-cell metabolic imaging reveals a SLC2A3-dependent glycolytic burst in motile endothelial cells. *Nat. Metab.* **3**, 714–727
75. Hong, J., Shin, J., Hong, J., and Shin, J. (2024) Prolonged Hypoxic Exposure Impairs Endothelial Functions: Possible Mechanism of HIF-1α Signaling. *Exerc. Sci.* **33**, 168–175

76. Alderfer, L., Russo, E., Archilla, A., Coe, B., and Hanjaya-Putra, D. (2021) Matrix stiffness primes lymphatic tube formation directed by vascular endothelial growth factor-C. *FASEB J.* **35**, e21498
77. DeBerardinis, R. J., Mancuso, A., Daikhin, E., Nissim, I., Yudkoff, M., Wehrli, S., and Thompson, C. B. (2007) Beyond aerobic glycolysis: Transformed cells can engage in glutamine metabolism that exceeds the requirement for protein and nucleotide synthesis. *Proc. Natl. Acad. Sci.* **104**, 19345–19350
78. Kim, B., Li, J., Jang, C., and Arany, Z. (2017) Glutamine fuels proliferation but not migration of endothelial cells. *EMBO J.* **36**, 2321–2333
79. Peyton, K. J., Liu, X., Yu, Y., Yates, B., Behnammanesh, G., and Durante, W. (2018) Glutaminase-1 Stimulates the Proliferation, Migration, and Survival of Human Endothelial Cells. *Biochem. Pharmacol.* **156**, 204–214
80. Wei, X., Wang, L., Xing, Z., Chen, P., He, X., Tuo, X., Su, H., Zhou, G., Liu, H., and Fan, Y. (2025) Glutamine synthetase accelerates re-endothelialization of vascular grafts by mitigating endothelial cell dysfunction in a rat model. *Biomaterials*. **314**, 122877
81. Durot, S., Doubleday, P. F., Schulla, L., Sabine, A., Petrova, T. V., and Zamboni, N. (2025) Multi-omics analysis of endothelial cells reveals the metabolic diversity that underlies endothelial cell functions. 10.1101/2025.03.03.641143
82. Han, F., Simeroth, S., Zhu, J., Gryniuk, I., Pranay, A., Chen, W., Wang, Y., Cai, Y., Shen, Z., Wang, G., Griffin, C. T., Xia, L., and Yu, P. (2025) Lymphatic endothelial mTORC1 instructs metabolic and developmental signaling during lymphangiogenesis. *Dev. Cell*. **60**, 2331-2347.e6
83. Meng, D., Yang, Q., Wang, H., Melick, C. H., Navlani, R., Frank, A. R., and Jewell, J. L. (2020) Glutamine and asparagine activate mTORC1 independently of Rag GTPases. *J. Biol. Chem.* **295**, 2890–2899
84. Tan, H. W. S., Sim, A. Y. L., and Long, Y. C. (2017) Glutamine metabolism regulates autophagy-dependent mTORC1 reactivation during amino acid starvation. *Nat. Commun.* **8**, 338
85. Durán, R. V., Oppliger, W., Robitaille, A. M., Heiserich, L., Skendaj, R., Gottlieb, E., and Hall, M. N. (2012) Glutaminolysis Activates Rag-mTORC1 Signaling. *Mol. Cell*. **47**, 349–358
86. Mullarky, E., and Cantley, L. C. (2015) Diverting Glycolysis to Combat Oxidative Stress. in *Innovative Medicine: Basic Research and Development* (Nakao, K., Minato, N., and Uemoto, S. eds), Springer, Tokyo, [online] http://www.ncbi.nlm.nih.gov/books/NBK500351/ (Accessed December 11, 2025)
87. Bergström, J., Fürst, P., Norée, L. O., and Vinnars, E. (1974) Intracellular free amino acid concentration in human muscle tissue. *J. Appl. Physiol.* **36**, 693–697
88. Cruzat, V., Macedo Rogero, M., Noel Keane, K., Curi, R., and Newsholme, P. (2018) Glutamine: Metabolism and Immune Function, Supplementation and Clinical Translation. *Nutrients*. **10**, 1564
89. Rodas, P. C., Rooyackers, O., Hebert, C., Norberg, Å., and Wernerman, J. (2012) Glutamine and glutathione at ICU admission in relation to outcome. *Clin. Sci.* **122**, 591–597